Characterization by Thermal Analysis of PP with Enhanced Biodegradability

L. CONTAT-RODRIGO, A. RIBES-GREUS, R. DÍAZ-CALLEJA

Department of Applied Thermodynamics, ETSIIV, Universidad Politéenica de Valencia, Apartado 22012, 465071 Valencia, Spain

Received 10 July 2000; accepted 25 February 2001

ABSTRACT: Samples of polypropylene (PP) filled with a biodegradable additive marketed under the Bioefect trademark, were subjected to an outdoor soil burial test for 21 months. Samples were initially characterized by thermogravimetry. The kynetics of the thermal degradation of both the carbonated chains of PP and the additive have been studied by means of the Hirata differential method and the Broido integral method. Such analysis reveals that the additive is more affected by the degradation process than the PP matrix. Changes in the morphology of the samples with the exposure time have been analyzed by Differential Scanning Calorimetry, in terms of the crystalline content of PP and its lamellar thickness distribution. The β- and α-relaxation zones of the dynamic mechanical relaxation spectra of both PP and pure Bioefect have been characterized using the Fuoss-Kirkwood equation and a deconvolution method. The analysis of the relaxation spectra shows that the interfacial and crystalline regions of the PP matrix are quite affected by the degradation process. On the other hand, it has also been found that changes in the crystallinity and the mechanical behavior of the samples take place in different stages. Such an evolution can be adequately represented by polynomial equations. © 2001 John Wiley & Sons, Inc. J Appl Polym Sci 82: 2174–2184, 2001

Key words: biodegradable additives; differential scanning calorimetry; dynamic-mechanical-thermal analysis; polypropylene; thermogravimetry

INTRODUCTION

Degradable polymers are designed to undergo changes in their chemical structure that lead to a loss of their physical properties, more rapidly than the inert polymers. Degradable polymers should preserve all their physical properties during their service life and, once discarded, they should degrade faster than a current plastic. In this sense, these materials can contribute to the reduction of plastics waste.

A certain degradability can be induced to polyolefins by simply incorporating into them a biodegradable additive in the form of a masterbatch.[1–8] Such additives are commonly made up of starch and other compounds that enhance degradadability and act as prooxidants.

The degradation mechanism of these materials is complex, because their environmental degradation results from the interaction of different oxidative processes (photo-oxidation, thermo-oxidation, biodegradation, etc.). It has been widely demonstrated that biodegradation of the polymeric matrix can only be carried out when its molecular weight has been reduced as a consequence of an abiotic oxidation.[9–13] Moreover, this abiotic oxidation determines the overall degradation rate of these materials, because biodegradation of polyolefins is a very slow process.[14,15]

Correspondence to: M. Amparo Ribes-Greus; e-mail: aribes@ter.upv.es.

Contract grant sponsor: Polytechnical University of Valencia.

Journal of Applied Polymer Science, Vol. 82, 2174–2184 (2001)

Table I Monthly Average Maximum Temperatures, T_{max} (°C), and Monthly Average Minimum Temperatures, T_{min} (°C), in Ayora (Valencia, Spain) during the Soil Burial Test

	January	February	March	April	May	June	July	August	September	October	November	December
							Year 1996					
T_{max}	13.6	13.2	16.3	20.9	23.8	29.8	33.0	31.8	25.2	23.2	17.0	12.9
T_{min}	6.7	2.8	5.5	7.9	11.0	14.7	17.6	18.4	13.9	9.8	7.5	5.2
							Year 1997					
T_{max}	11.5	17.7	21.2	21.8	23.8	27.6	30.6	32.2	28.0	24.3	16.6	13.1
T_{min}	5.2	4.3	3.7	8.5	12.2	15.7	15.9	17.5	16.0	12.4	9.1	5.6
							Year 1998					
T_{max}	13.1	16.0	21.1	19.4	22.0	30.2	34.8	34.3	28.2	23.6	17.4	12.7
T_{min}	4.8	4.3	5.4	8.1	10.5	15.7	18.6	17.8	17.0	9.0	6.0	0.4

Degradation of polyolefins with enhanced biodegradability leads to both chemical and physical changes in the polymeric matrix. For that reason, changes in the structural, morphological, and mechanical properties of such polyolefins should be analyzed to try to elucidate the mechanism of their degradation process.

The objective of this work is to characterize by thermal analysis the changes undergone by samples of PP with enhanced biodegradability, subjected to an outdoor soil burial test to evaluate their use as seedboxes.

EXPERIMENTAL

Materials

Polypropylene 1148-TC (PP) supplied by BASF (Germany) was used as the polymeric matrix. Bioefect 72000 from Proquimaq Color, S.L. (Spain) was used as biodegradable additive. Bioefect combines starch and other compounds that promote biodegradation, but its exact composition is undisclosed.

Samples

Samples of PP containing 10% by weight of Bioefect have been processed by injection as seedboxes.

Samples of pure Bioefect have also been prepared by compression moulding with a Carver M press.

Soil Burial Test

The seedboxes were subjected to an outdoor soil burial test in Ayora (Valencia, Spain) for 21 months. Average temperatures at this place during the test are summarized in Table I.

Samples were removed after different periods of time of 0, 3, 6, 9, 12, 15, and 21 months. After removal, they were carefully washed with a soap solution to stop the biodegradation process, and dried with a piece of paper before being analyzed.

The soil used in this test is a mixture of 50% Finnish peat, 25% coconut fiber, and 25% pine bark. This composition is typically employed in seedbeds for pine trees growth. The pH of this soil (measured in water) has a value of 6.75.

Thermogravimetric Measurements

Thermogravimetric analysis of the undegraded seedboxes and those degraded in soil for 12 and 21 months was carried out by means of a Mettler TGA/SDTA 851 module. Dynamic measurements were performed from 25 to 600°C at a heating rate of 10°C/min under argon atmosphere (flow rate = 200 ml/min). The samples masses were about 10 mg.

The thermodegradation products were analysed with a Balzers Thermostar mass spectrometer connected to the TGA analyzer.

Scans of all the molecules with molecular weights between 0 and 200 u.m.a were analyzed.

Differential Scanning Calorimetry Measurements

The crystallinity of the samples was studied by Differential Scanning Calorimetry (DSC). Both the crystalline content and the melting temperature were measured with a Perkin-Elmer DSC-4 calorimeter, previously calibrated with indium. A total of 5–6 mg of samples were weighed out in a standard aluminium pan. The sealed pans were scanned at a heating rate of 10°C/min form 0 to 200°C under nitrogen atmosphere.

Dynamic Mechanical Measurements

The viscoelastic properties were determined by means of a Polymer Laboratories Ltd (now Rheo-

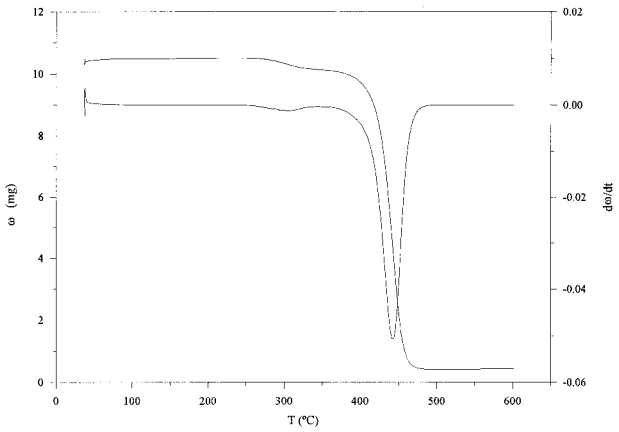

Figure 1 TG and DTG curves of the undergraded seedbox.

metrics) Dynamic Mechanical Thermal Analyzer, MARK II DMTA. Deformation was applied in the cantilever double-clamping flexure mode. The storage modulus, E' and the loss tangent, tan δ were measured from −80 to 160°C at the frequencies of 0.3, 1, 3, 10, and 30 Hz with a heating rate of 1°C/min.

RESULTS AND DISCUSSION

Thermogravimetry

Samples have been initially characterized by thermogravimetric analysis.

It has been found that samples of PP filled with the Bioefect additive display two weight loss zones regardless of the exposure time in soil (Fig. 1). The characteristic parameters of each of these stages are shown in Table II.

According to these parameters, the first stage, with maximum around 300°C, has been assigned to the degradation of the starch[1] and other products contained in the additive, which percentage is never greater than 2%.

The other degradation zone, where the maximum is located around 442°C, corresponds to the main stage of the process. Such a stage has been attributed to the complete thermodegradation of the carbonated chains of PP.

The characteristic parameters of the main stage remain basically the same as the degradation time in soil increases. However, both the mass loss and the temperature of the maximum associated to the first stage initially decrease and increase afterwards.

The residue remains basically unaltered during the degradation process.

Activation energies of both thermodegradation zones have been determined using different mathematical models.

Hirata describes the kynetics of a system undergoing chemical changes in terms of the weight of the sample at time t, ω:[16]

$$\frac{d\omega}{dt} = -k(T) \cdot \omega \tag{1}$$

where k is the constant of the rate of reaction, which is dependent on temperature. Such dependence is generally expressed by means of the Arrhenius equation:

$$k(T) = A \exp\left(\frac{-E}{RT}\right) \tag{2}$$

where R is the gas constant, T is the absolute temperature, E is the activation energy, and A is the preexponential factor.

Substituting the Arrhenius equation in eq. (1) and taking logarithms, it results the Hirata equation:

$$\ln\left(-\frac{d\omega}{dt}\right) - \ln \omega = \ln A - \frac{E}{RT} \tag{3}$$

Table II Characteristic Parameters of the Thermal Degradation as a Function of the Exposure Time in Soil

Exposure Time (Months)	Mass Loss (%)	Residue (%)	Mass Loss First Stage (%)	Mass Loss Main Stage (%)	T-Peak First Stage	T-Peak Main Stage (°C)
0	96.2	3.8	2.1	90.2	305.9	442.0
12	95.7	4.3	0.3	981.0	297.8	441.5
21	95.7	4.3	1.6	90.9	304.2	441.7

Table III Activation Energies Calculated with the Hirata Differential Method as a Function of the Exposure Time in Soil

Exposure Time (Months)	T (°C)	E_a (kcal/mol)	T (°C)	E_a (kcal/mol)	T (°C)	E_a (kcal/mol)	T (°C)	E_a (kcal/mol)
0	412–446	84.4	360–412	49.6	276–298	17.6	251–273	56.6
12	412–446	84.6	360–412	48.4	279–302	9.5	256–279	43.5
21	412–446	81.9	360–412	50.4	276–298	16.5	240–273	50.7

The plot of $[\ln(-d\omega/dt) - \ln\pi]$ vs. the reciprocal of temperature should give a straight line for each process, from which the activation energy and the preexponential factor can be calculated.

The Hirata model is a differential method, because it is directly deduced from a kinetic function in terms of derivatives.

The activation energies calculated with this model are summarized in Table III. Two kinds of processes, with different activation energies, have been found to be involved in the thermal degradation of both the carbonated chains of PP (446–360°C) and the additive (250–300°C). The results show small changes in the activation energies associated to the decomposition of the carbonated chains. However, the activation energies corresponding to the thermodegradation of the additive exhibit more significant changes as a function of the exposure time. These activation energies display a decrease and a later increase.

On the other hand, the kinetics of a system undergoing chemical changes is usually also expressed in the form:

$$\frac{d\alpha}{dt} = f(\alpha)k(T) \tag{4}$$

where the rate of change the conversion α, with respect to time t, is equated to separable functions of α and the absolute temperature T.

The conversion or reacted fraction α, can be defined as the weight loss at time t, divided by the weight loss at infinite time or total weight loss:

$$\alpha = \frac{\omega_o - \omega}{\omega_o - \omega_\infty} \tag{5}$$

Polymer degradation often consists in chain reactions. Thus, $f(\alpha)$ representing the net result of a series of elementary steps. Each elementary step has its own activation energy, which makes each step to respond differently to temperature changes.

The temperature dependence of the rate of reaction is generally expressed by means of the Arrhenius equation.

The simplest model used to describe the kinetic function $f(\alpha)$ is:

$$f(\alpha) = (1 - \alpha)^n \tag{6}$$

where n is the apparent order of reaction.

Thus, substituting $f(\alpha)$ and $k(T)$ by their expressions in eq. (4):

$$\frac{d\alpha}{dt} = (1 - \alpha)^n A \exp\left(\frac{-E}{RT}\right) \tag{7}$$

The initial condition of $\alpha = 0$ at $T = T_0$ leads to the following integral form:

$$\int_0^\alpha \frac{d\alpha}{(1 - \alpha)^n} = \frac{A}{\beta} \cdot \int_{T_0}^T \exp\left(\frac{-E}{RT}\right) \cdot dT \tag{8}$$

where β is the heating rate used in the thermogravimetric analysis, ($\beta = dT/dt$).

The integral methods are based on this equation. The one proposed by Broido has also been used to analyze the kinetics of the two stages in terms of their activation energy:[17]

$$\ln\ln\left(\frac{1}{x}\right) \cong -\frac{E}{RT} + \text{const} \tag{9}$$

where x is the residual fraction defined as:

$$x = 1 - \alpha = \frac{\omega - \omega_\infty}{\omega_0 - \omega_\infty} \tag{10}$$

The Broido integral method has only allowed the kinetic study of the degradation of the carbonated

Table IV Activation Energies Calculated with the Broido Integral Method as a Function of the Exposure Time in Soil

Exposure Time (Months)	T (°C)	E_a (kcal/mol)	T (°C)	E_a (kcal/mol)
0	453–476	50.7	422–448	76.8
12	453–476	53.4	422–448	80.5
21	453–476	50.0	422–448	76.9

chains of PP. For such a method, the zone corresponding to the thermal degradation of the additive is not as clearly defined as it was in the case of the Hirata differential method.

The activation energies estimated with the Broido equation for the different processes involved in the decomposition of the carbonated chains are shown in Table IV.

Two different processes have also been found. The one from 422 to 448°C was already detected with the Hirata model. Similar results have been obtained for this stage with the Broido and the Hirata equations. However, the Broido differential method has allowed the identification of a third process at higher temperatures (453–476°C) involved in the thermodegradation of PP.

Thus, the integral methods, like that of Broido, seem to better define the high-temperature zone, while the differential methods, like that of Hirata, seems to better describe the low-temperature zone.

Nevertheless, for a same degradation stage, both kinds of methods lead to similar values of the activation energies.

On the other hand, the thermogravimetric results reveal that the additive is more affected by the degradation process than the polymeric matrix.

From the mass spectrometry analysis of the thermodegradation products, volatile compounds with the following molecular weights have been identified: 2, 14–21, 28, 32, 34, 40, 44.

These results indicate that the thermodegradation of the samples has been complete, because only very low molecular weight products such water, carbon monoxide, and carbon dioxide have been identified. This can be due to the presence of a prooxidant in the additive, that could have favored the complete thermal decomposition of the polymeric matrix.

DSC

Changes in the crystallinity of the samples with the exposure time have been studied by DSC.

In the DSC thermogram of pure Bioefect, an endotherm around 108°C appears, which has been attributed to the presence of polyethylene in its composition (Fig. 2).

The DSC thermograms of the seedboxes display a main endotherm that has been assigned to PP (Fig. 3). A smaller endothermic peak located at lower temperatures has been associated to Bioefect, because its location correlates well with that observed in the DSC curve of this additive.

Melting temperatures have been directly obtained from the thermograms. Values around 166°C have been found for all the samples, regardless of the exposure time. Thus, during the degradation process in soil, no significant changes of the melting temperature of PP occur [Fig. 4(a)].

The total crystalline content of PP in the samples has been calculated according to the following equation:

$$X = \frac{(H_a - H_c)}{H_m} \tag{11}$$

where, H_a and H_c are the enthalpies in the melt state and the crystalline state, respectively. Their difference is directly obtained from the thermo-

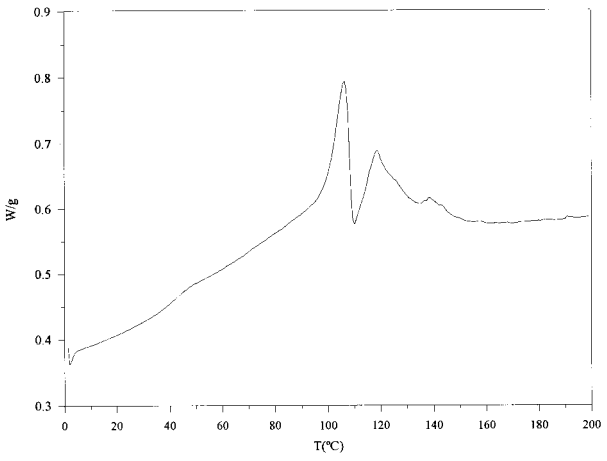

Figure 2 DSC thermogram of Bioefect 72000.

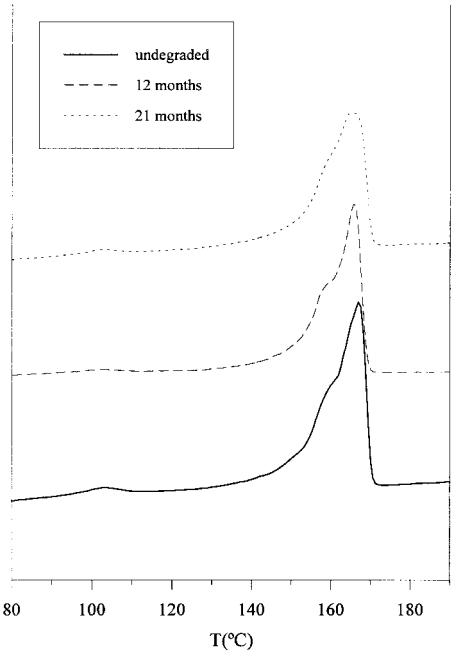

Figure 3 DSC thermograms of the seedboxes after different exposure times in soil.

gram. H_m is the change in the melting enthalpy of a perfect crystal of infinite size. For PP, H_m = 50 cal/g ≈ 209 J/g.[18]

It has been found that the evolution of the crystalline content of PP with the degradation time can be adequately represented by a polynomial equation [Fig. 4(b)]. Similar results have been obtained by Hamid et al. for the evolution of the elongation at break with the exposure of LDPE films subjected to weathering.[19–20]

On the other hand, such an evolution confirms that changes in crystallinity take place in different stages, as suggested by Albertsson et al.[21] In this case, the crystalline content increases initially. Afterwards, it decreases and then it shows a slight tendency to increase again.

In semicrystalline polymers, degradation starts in the amorphous phase and the interfacial regions, in which oxygen is soluble. This could explain the initial increase of crystallinity. As degradation takes place, the crystalline phase begins to disintegrate, thus reducing the crystalline content of the polymer.

On the other hand, Hawkins suggests that the crystalline content of a semicrystalline polymer is conditioned by the amorphous phase that restricts the crystallization process.[22] A scission of the molecules of the amorphous regions, caused for example by oxidation, allows the crystallization to proceed to a higher extent. Such an increase in crystallinity could be then considered as degradation.

The lamellar thickness distribution of PP in the samples has been determined according to the procedure proposed by Eder:[23]

Eder considers that the flow rate of the heat of fusion at a given temperature, given by the deflection of the DSC trace from the baseline, is directly proportional to the fraction of lamellae with this melting point.

The Thomson equation gives the relationship between the lamella thickness, l, and the melting temperature of lamellae of thickness l:

$$T_m = T_m^\circ \cdot \left(1 - \frac{2\sigma_e}{\Delta h_m \cdot 1}\right) \tag{12}$$

where T_m is the melting temperature of lamellae of thickness l; T_m° is the equilibrium melting temperature of an infinite crystal; σ_e is the surface free energy of the basal plane; Δh_m is the enthalpy of fusion per unit volume; and l is the lamellae thickness.

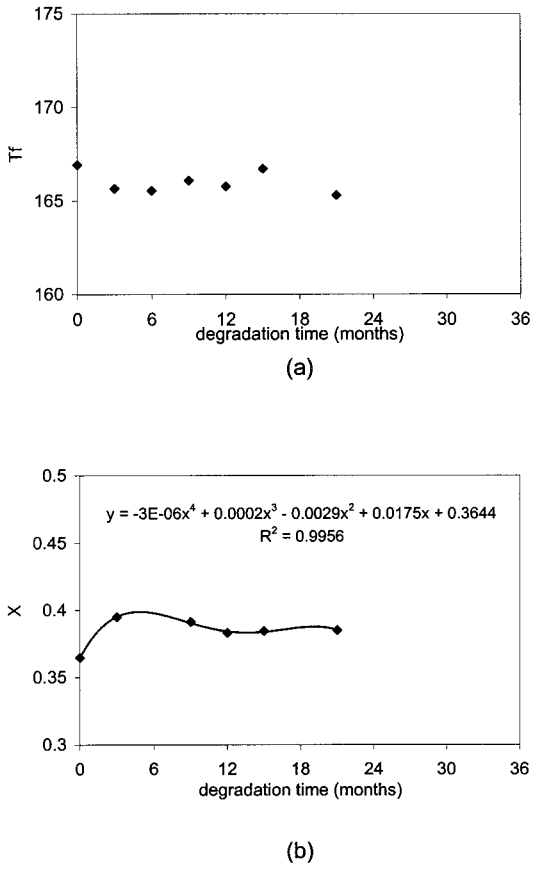

Figure 4 Evolution of (a) the melting temperature and (b) the crystalline content of PP with the exposure time in soil.

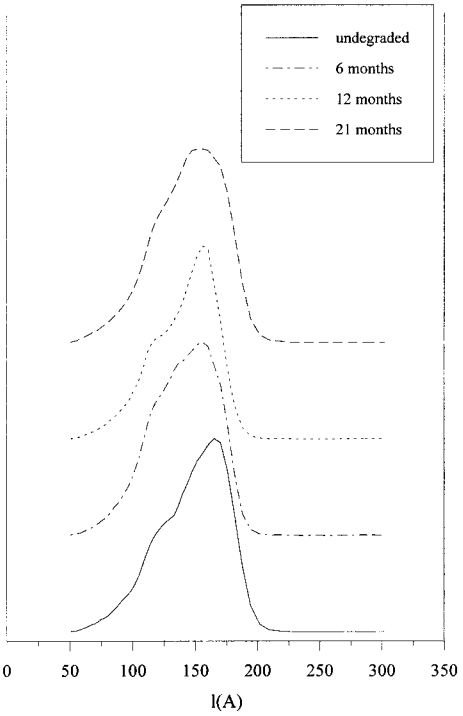

Figure 5 Lamellar thickness distribution of PP after different exposure times in soil.

According to this equation, Eder assumes that at a given temperature for a sample of molten polymer, the rate of heat consumption is proportional to the fraction of lamellae whose thickness is given by the Thomson equation.

Thus, the plot of the normalized deflection against lamella thickness, l, corresponding to the temperature, T, as calculated from the Thomson equation, yields the distribution curve of lamellae thicknesses.

The lamellar thickness distribution of PP in the undegraded sample and the samples degraded for 6, 12, and 21 months has been determined (Fig. 5). The lamellar thickness distribution of PP covers thicknesses up to 200 Å. During the degradation process, successive broadenings and narrowings of the distribution are observed.

DMTA

The viscoelastic behavior of the samples during the degradation process in soil has also been studied.

Figure 6 shows the mechanical relaxation spectrum of pure Bioefect in terms of the storage modulus, E', and the loss tangent, tan δ. This biodegradable additive presents the typical spectrum of a low-density polyethylene (LDPE), displaying the β and α-relaxation zones. This confirms the presence of such polyolefin in the formulation of Bioefect, as it was already suggested from its DSC thermogram.

Each of the relaxation zones of pure Biofect has been characterized following the Fuoss-Kirkwood empirical model:

$$E'' = \frac{E''_{\max}}{\cosh m \dfrac{E_a}{R}\left(\dfrac{1}{T} - \dfrac{1}{T_m}\right)} \tag{13}$$

where $E''_{\max}$ is the maximum of the loss modulus; m is the Fuoss-Kirkwood parameter; and T_m is the temperature of the maximum of the loss modulus.

Because the β- and α-relaxations overlap, the deconvolution method proposed by Charlesworth has been applied.[24] This consists in considering the experimental data of the loss modulus as the sum of each of these contributions:

$$E'' = \sum_{i=1}^{n} E_i \tag{14}$$

Figure 7 shows the deconvolution of the different overlapped contributions for the Bioefect additive. The β-relaxation has been separated from the α-relaxation zone. This latter has been decomposed into three subrelaxations called α_{I}, α_{II}, and α_{III} in order of increasing temperature.

The characterization of the relaxations has been completed with the estimation of the apparent activation energy, E_a, of each of the identified relaxations. These have been calculated by fitting the dependence of the mean relaxation times on the temperature to the Arrhenius equation:

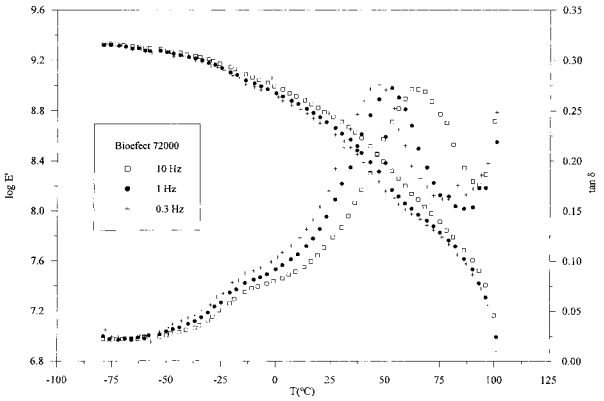

Figure 6 Plot of E' and tan δ vs. temperature for Bioefect 72000 at different frequencies.

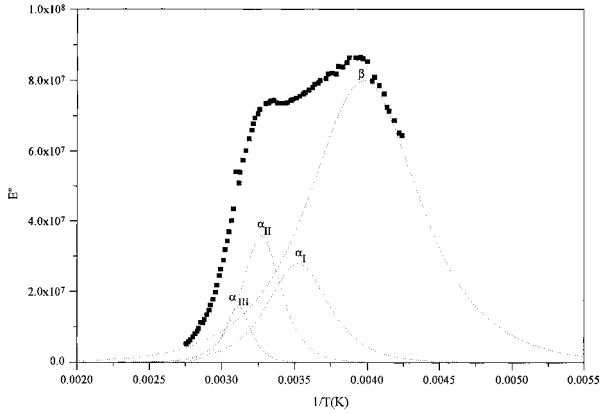

Figure 7 Deconvolution in terms of E″ of the β- and α-relaxations of Bioefect 72000 at 1 Hz of frequency.

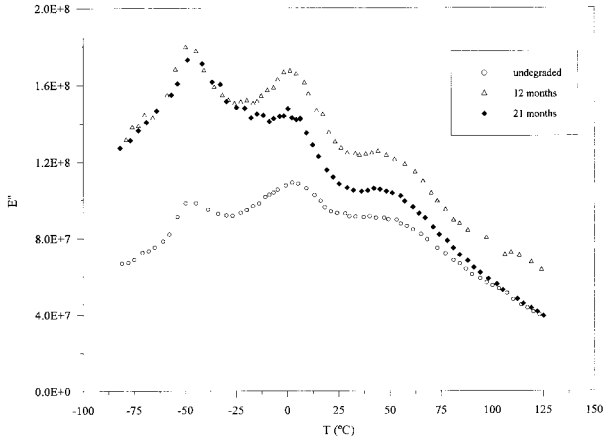

Figure 8 Plot of E'' vs. temperature for the seedboxes degraded in soil for different periods of time.

$$\ln f_m = \ln f_0 - \frac{E_a}{R} \cdot \frac{1}{T_m} \tag{15}$$

where, T_m and f_m are, respectively, the temperature and the frequency of the maximum of the loss modulus.

Values of the activation energy around 60 kcal/mol for the β-relaxation and around 40–60 kcal/mol for the α-relaxations of Bioefect have been obtained (Table V).

The mechanical relaxation spectrum of the seedboxes as a function of the exposure time is shown in Figure 8. The spectra basically exhibit the β- and α-elaxation zones typical of PP. The characteristic relaxations of the additive are not explicitly observed in these spectra, because its concentration in the blend is quite low (10% by weight), and its relaxations occur at very similar temperatures to those of PP, overlapping them.

It has been established that the α-relaxation of PP is associated to molecular motions occurring in the crystalline phase.[25,26] The β-relaxation of PP may result from movements of the molecular chains that form the crystalline–amorphous interface.

Table V Apparent Activation Energies, E_a, of the Relaxations of Bioefect 72000

Relaxation	E_a (kcal/mol)
$_{III}\beta$	57.8
α_I	47.4
α_{II}	60.5
α_{III}	41.7

Figure 8 also shows during degradation in soil, an initial increase of the loss modulus of the seedboxes, followed by a later tendency to decrease.

On the other hand, the spectra of the seedboxes have been characterized following the deconvolution method previously described, together with the Fuoss-Kirkwood equation.

A β-relaxation and two α-relaxations, called α_I, α_{II} in order of increasing temperature have been identified (Fig. 9). These relaxations result from the overlapping of the contributions of PP and those of Bioefect.

The evolution with the exposure time of the temperature of the maximum, T_m, and the m Fuoss-Kirkwood parameter calculated for each relaxation is plotted in Figures 10 and 11, respectively.

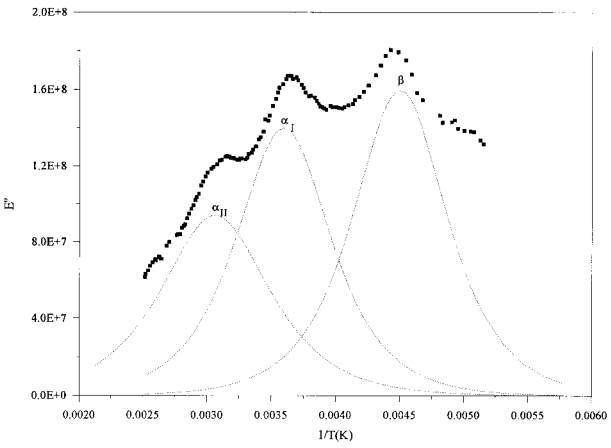

Figure 9 Deconvolution in terms of E'' and at 1 Hz of frequency of the β- and α-relaxations of the seedbox degraded in soil for 12 months.

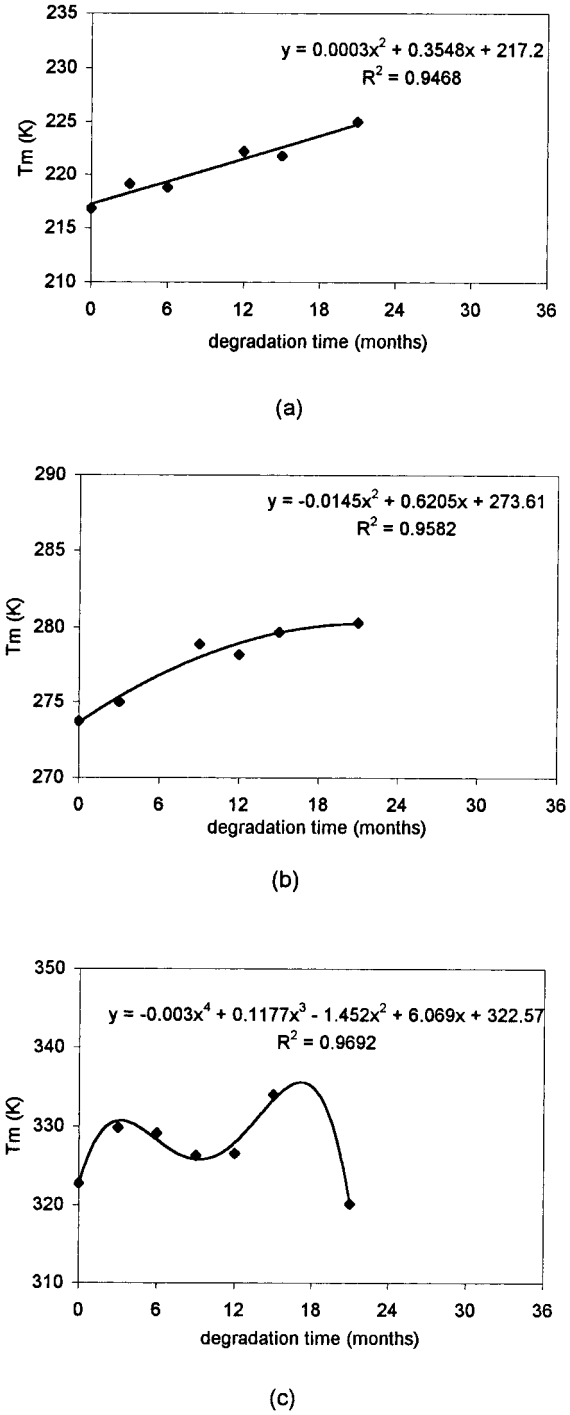

Figure 10 Evolution with the exposure time of the temperature of the maximum of the loss modulus, T_m, of the (a) β, (b) α_I, and (c) α_{II} relaxations of the seedboxes.

It has been found that the evolution of these parameters can be adequately represented by polynomial equations. Such an evolution was also undergone by crystallinity of PP. This confirms the idea that biodegradation is a complex process that takes place in different stages.[21]

During the 21 months of exposure, T_m increases with the degradation time for both the β- and α_I relaxations (Fig. 10). However, for this latter the

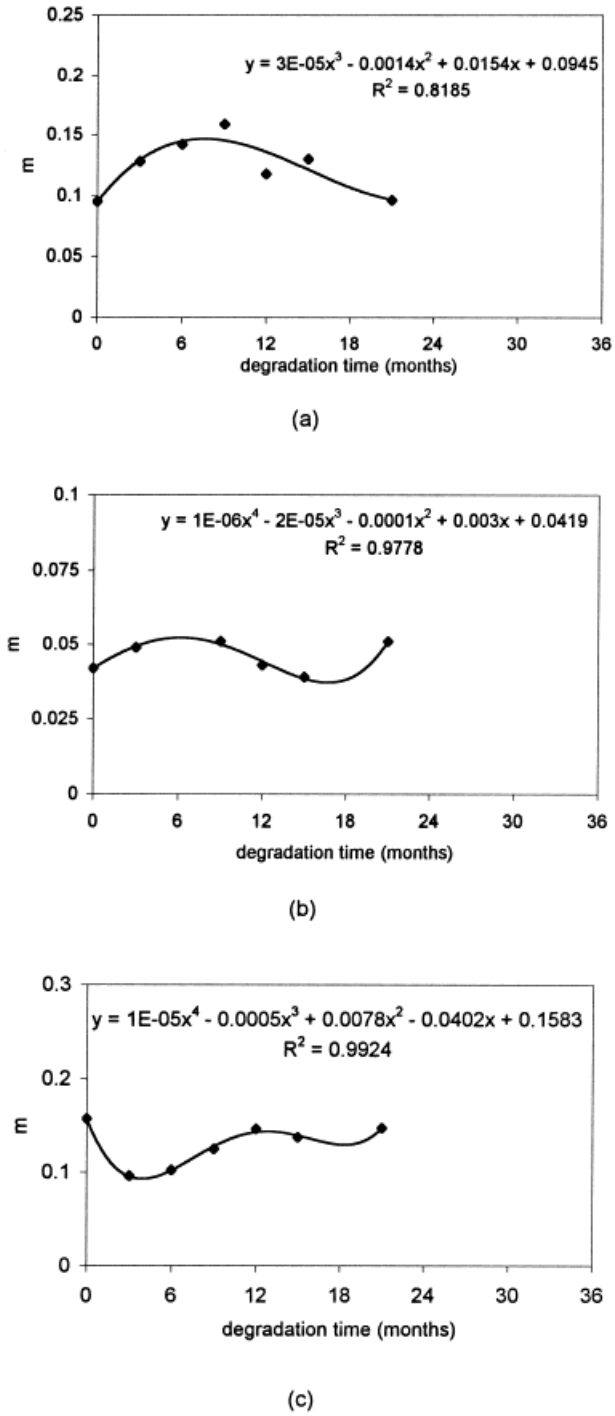

Figure 11 Evolution with the exposure time of the m Fuoss-Kirkwood parameter, m, of the (a) β, (b) α_I, and (c) α_{II} relaxations of the seedboxes.

tendency is more gradual. More significant changes are observed for the α_{II} relaxation. For this relaxation, T_m increases and decreases successively during the degradation test. Assuming that this relaxation is related to motions of the molecular chains in the crystalline phase, this indicates that such phase is quite affected by the degradation process.

Because oxygen is insoluble in the crystalline regions of polyolefins, it cannot be expected that degradation starts in this phase. However, the results show that changes in other regions significantly affects the crystalline content.

The m Fuoss-Kirkwood parameter is related to the relaxation width. Figure 11 shows out-of-phase evolutions of this parameter for the β- and α-relaxations. For all of them, an initial increase of the m parameter, followed by a later decrease is noted.

Figure 12 displays the evolution with the exposure time of the activation energies of the relaxations of the seedboxes, calculated with the Arrhenius equation. In every case, this evolution can be fitted to polynomial equations, thus proving that, in general, changes in the mechanical behavior of samples subjected to an outdoor soil burial test follow different stages, as did changes in crystallinity.

The activation energy of the β-relaxation of the undegraded seedbox is around 66 kcal/mol. It is observed that such parameter exhibits a marked decrease during the first 3 months of degradation in soil. Afterwards, it increases and decreases successively. However, the activation energy of the degraded samples always remains lower than that of the undegraded sample.

Assuming that the β-relaxation of polyolefins is related to movements in the interfacial regions, this fact indicates that degradation leads to a greater mobility of the chains located in these regions. Because oxygen is soluble in the amorphous phase and crystalline–amorphous interface, it can be expected that degradation begins in these regions. This could cause the decrease in the activation energy of the β-relaxation.

On the other hand, values between 100–200 kcal/mol for the activation energy of the α_I relaxation of the seedboxes have been obtained. Such high values of the activation energy suggest that the α_I relaxation can be associated to cooperative movements of the molecular chains that form the amorphous and interfacial regions, similar to the glass transition of amorphous polymers. In this sense, such kinds of movements could originate motions in the crystalline phase itself, which will result in the α_{II} relaxation.

After decreasing during the first 9 months of exposure, the activation energy of the α_I relaxation increases significantly. Finally, a tendency to decrease is observed.

Concerning the α_{II} relaxation of the seedboxes, an activation energy of about 30 kcal/mol has

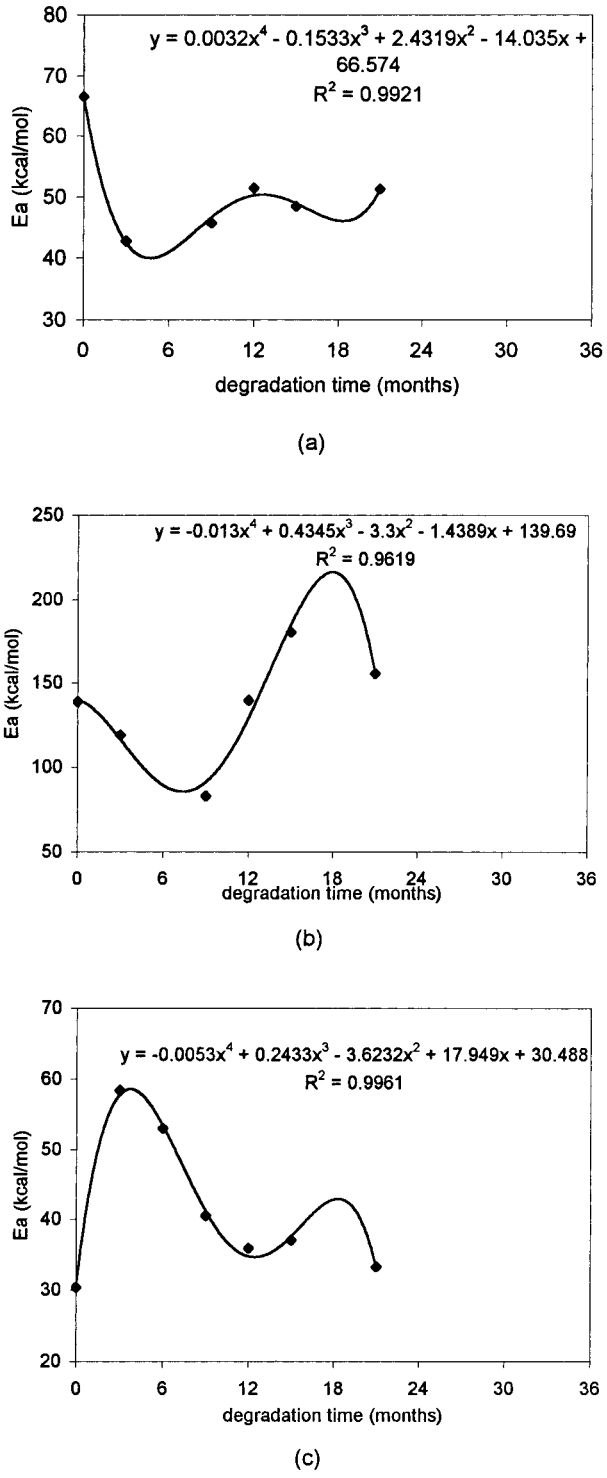

Figure 12 Evolution with the exposure time of the apparent activation energies, E_a, of the (a) β, (b) α_I, (c) α_{II} relaxations of the seedboxes.

been obtained for the undegraded sample. During the degradation process, the activation energy of this relaxation exhibits significant changes, displaying values from 30 to almost 60 kcal/mol. This proves again that the crystalline phase is also quite affected by degradation.

Furthermore, it is observed that the activation energy of the α_{II} relaxation follows a parallel evolution in time to that previously noted for the crystalline content of PP. An increase in crystallinity leads to higher activation energies, whereas a decrease in the crystalline content of PP causes a decrease in the activation energy. It is also noted that small changes in crystallinity leads to more marked changes in the activation energy.

This supports the idea that the α_{II} relaxation is related to motions of the molecular chains in the crystalline regions.

CONCLUSIONS

The thermogravimetric results have shown that the additive Bioefect is more affected by the degradation process in soil than the PP matrix.

The evolution with the exposure time in soil of the crystalline content of PP, as well as that of the m Fuoss-Kirkwood parameter, the temperature of the maximum of the relaxation and the activation energy of each of the mechanical relaxations can be adequately represented by polynomial equations. This indicates that changes in both crystallinity and the mechanical behavior of samples subjected to an outdoor soil burial test take place in different stages.

This result confirms the idea suggested by Albertsson et al., that biodegradation is a complex process that develops in different phases.

The analysis of the relaxation spectra shows that the degradation process significantly affects the interfacial regions of PP, as demonstrated by the changes produced in the characteristic parameters of the β-relaxation.

Although the oxygen is usually insoluble in the crystalline phase and degradation cannot be expected to be initiated in this phase, changes occurring in the amorphous–crystalline interface due to the degradation process significantly affect the crystalline phase. The α_{II} relaxation exhibits noticeable changes that correlate well with the calorimetric results.

The authors are grateful for the financial support received for this work from the Polytechnical University of Valencia via a project of the "Programa de Incentivo a la Investigación de la UPV. Ayuda para Grupos Interdisciplinares."

REFERENCES

1. Griffin, G. J. L., Ed. Chemistry and Technology of Biodegradable Polymers; Blackie Academic & Professional: Glasgow, 1994.
2. Chiellini, E.; Solaro, R.; Corti, A.; Picci, G.; Leporini, C.;Pera, A.; Vallini, G.; Donaggio, G. Chim Indust 1991, 8, 656.
3. Albertsson, A.-C.; Barenstedt, C.; Karlsson, S. J Environ Polym Degrad 1993, 1, 241.
4. Johnson, K. E.; Pometto, A. L., III; Nikolov, Z. L. Appl Environ Microbiol 1993, 59, 1155.
5. Albertsson, A. C.; Barenstedt, C.; Karlsson, S. J Appl Polym Sci 1994, 51, 1097.
6. Greizerstein, H. B.; Syracuse, J. A.; Kostyniak, P. J.. Polym Degrad Stabil 1993, 39, 251.
7. Bastioli, C. Polym Degrad Stabil 1998, 59, 263.
8. Bastioli, C.; Degli Innocenti, F.; Guanella, I.; Romano, G. In Degradable Polymers, Recycling and Plastic Waste Management; Albertsson, A. C.; Huang; S. J., Eds. Marcel Dekker: New York, 1995, p. 247.
9. Gage, P. Tappi J 1990, October, 161.
10. Hakkarainen, M.; Albertsson, A.-C.; Karlsson, S. J Appl Polym Sci 1997, 66, 959.
11. Sastry, P. K.; Satyanarayana, D.; Mohan Rao, D. V. J Appl Polym Sci 1998, 70, 2251.
12. Albertsson, A. C.; Barenstedt, C.; Karlsson, S. Polym Degrad Stabil 1992, 37, 163.
13. Erlandsson, B.; Karlsson, S.; Albertsson, A. C. Polym Degrad Stabil 1997, 55, 237.
14. Schnabel, W. Polymer Degradation, Principles and Practical Applications; Hanser Publishers: München, 1992.
15. Ohtake, Y.; Kobayashi, T.; Asabe, H.; Murakami, N.; Ono, K. J Appl Polym Sci 1998, 70, 1643.
16. Hirata, T.; Werner, K. E. J Appl Polym Sci 1987, 33, 1533.
17. Broido, A.; J Polym Sci Part A 1969, 27, 1761.
18. Turi, E. Thermal Characterization of Polymeric Materials; Academic Press: New York, 1997, vols. I and II.
19. Amin, M.-B.; Hamid, S. H.; Rahman, R. J Appl Polym Sci 1995, 56, 279.
20. Hamid, S. H.; Amin, M. B. J Appl Polym Sci 1995, 55, 1385.
21. Albertsson, A.-C.; Karlsson, S. Prog Polym Sci 1990, 15, 177.
22. Hawkins, W. Polymer Degradation Stabilization; Springer-Verlag: Berlin, 1984.
23. Wochowicz, A.; Eder, M. Polymer 1984, 25, 1268.
24. Charlesworth, J. M. J Mater Sci 1993, 28, 399.
25. McCrum, N. G.; Read, E.; Williams, G. Anelastic and Dielectric Effects in Polymeric Solids; Dover Pulications: New York, 1967.
26. Riande, E.; Díaz-Calleja, R.; Prolongo, M. G.; Masegosa, R. M.; Salom, S. Polymer Viscoelasticity. Stress and Strain in Practice; Marcel Dekker Inc.: New York, 2000.